



1 **Land formation driven by sediment accumulation and vegetation dynamics in the marsh: A case study**
2 **in the Kitchen Pond area in the modern Mississippi River Delta.**

3

4 Janaka Wijayawardhana^{1*}, Christian James¹, Aaron Jordan¹, Harish Ratnayaka^{1*}.

5 ¹Xavier University of Louisiana, Drexel Dr, New Orleans, LA 70125, United States.

6 **Corresponding Authors : jwijayaw@xula.edu, hратnaya@xula.edu, Tel. (504)520-7527, (504)520-5709.*

7

8

9

10

11

12

13

14

15

16

17

18

19

20

21

22

23

24

25

26

27

28

29

30

31

32

33

34

35

36

37

38

39

40

41



42 **Abstract**

43 A study was conducted to analyze how sediment accumulation affects land formation and marsh
44 development in river deltaic ecosystems. It examined the temporal variations in turbidity levels and
45 chlorophyll content driven by sediment input, and their long-term impacts on land formation processes
46 in the Kitchen Pond area of the modern Mississippi River Delta. Using multi-temporal Landsat imagery
47 (2006–2021) and spectral indices such as NDWI (Normalized Difference Water Index), NDTI (Normalized
48 Difference Turbidity Index), and NDCI (Normalized Difference Chlorophyll Index), the current analysis
49 demonstrated the evolution of a new bird-foot deltaic pattern within ecosystems with similar
50 morphology. Nearly a 15-year period was needed to form a permanent landmass by the sedimentation
51 process under the conditions. A mathematical model was also developed to predict actual turbidity levels
52 in waterbodies using remote sensing data. This study shows the interconnected relationship between
53 sediment deposition, vegetation growth, and their combined influence on the emergence of new land.
54 These findings offer valuable insights to the restoration agencies for developing effective strategies and
55 adaptive management approaches for similar environments.

56 **Key words:** Land formation, Marsh development, Mississippi River Delta, Remote sensing

57 **1. Introduction**

58 Sediment accumulation is an important mechanism of land formation and marsh development in river
59 deltaic ecosystems. This phenomenon is especially pronounced in the Mississippi River Delta (MRD),
60 where the deposition of organic and mineral sediments influences the reshaping of the delta's
61 morphology (Sanks et al., 2022). The typical "bird-foot" morphology of the modern/lower Mississippi River
62 Delta is primarily a result of sediment delivery by river flow. It is often emphasized that this process
63 outweighs the effects of waves and tidal reworking. As a result, narrow distributary channels are extended
64 into the Gulf of Mexico. Due to this, finger-like landforms develop, creating the distinctive delta shape
65 (Edmonds and Slingerland, 2007; Syvitski and Saito, 2007). Such land formations often occur when high
66 sediment loads are delivered to relatively flatter areas, allowing sediment to accumulate at low laying
67 areas of the river and form distributary channels independently.

68 During the seasons with high floods, a large amount of essential nutrients is delivered to the marsh
69 through sediment carried by the river, supporting the growth of algae and aquatic plants (Amer et al.,
70 2017). Elevated chlorophyll levels in water bodies reflect this process, indicating nutrient richness and
71 increased biomass within the ecosystem (Xu et al., 2022). However, investigating these dynamics has
72 certain challenges, as the identification of the precise starting point or triggering point of ecosystem
73 changes under natural conditions is often difficult. In such cases, man-made structures can serve as
74 reference points for ecosystem alterations. For example, in 2006-2007, a diversion canal was constructed
75 in the Kitchen Pond area of the modern MRD (bird-foot delta). This incident can be considered an ideal
76 case study for examining how sediment deposition affects aquatic chlorophyll levels, turbidity, and land
77 formation processes within a similar water body. Satellite imagery serves as an invaluable tool in this type
78 of analysis, enabling long-term monitoring of environmental changes and their impacts (USGS, 2006;
79 Barras, 2006).

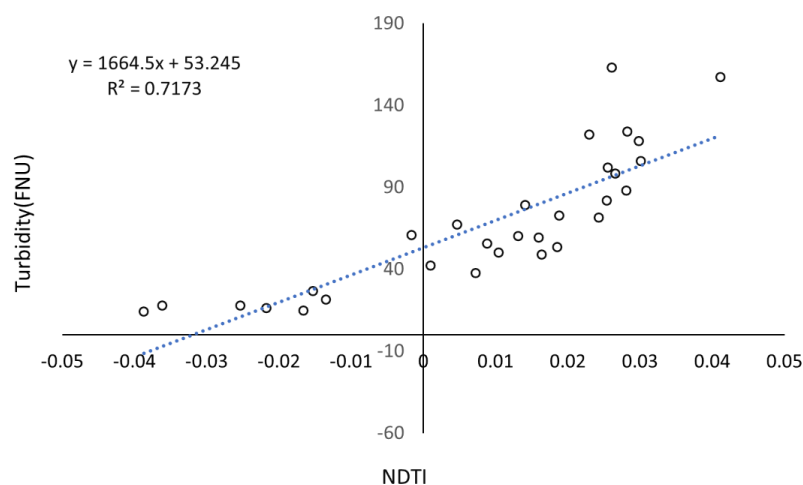
80 Sediment-vegetation feedback mechanisms and their implications for sustainability and restoration of
81 deltaic ecosystems have been demonstrated by recent research. For instance, Schile et al. (2014), Kirwan
82 and Megonigal,(2013) showed that the vegetation grows in response to sediment deposition and
83 promotes further sediment capture, thereby creating a self-reinforcing cycle that is crucial for both



84 formation and stability of marsh. However, the persistence of these landforms is not guaranteed, as
85 external pressures such as accelerated sea-level rise, subsidence, reduced sediment loads in future etc.,
86 can threaten newly formed marshes and even reverse land gains (Kearney et al., 2002). The application
87 of remote sensing, particularly with multi-temporal satellite imagery and advanced indices, has become
88 indispensable for tracking these complex processes over time and at landscape scales (Kuenzer et al.,
89 2011). Multi-temporal satellite imagery, combined with spectral indices such as NDWI, NDTI, and NDCI,
90 enables researchers to monitor changes in the extent of water, sediment deposition, and vegetation
91 dynamics with high temporal and spatial resolution (Kuenzer et al., 2011; McFeeters, 1996). This imagery
92 is crucial for understanding the physical processes that drive the changes of the geomorphology of the
93 modern MRD (bird-foot region), whereby long-term sustainability of this wetland system of enormous
94 ecological and economic significance. Thus, the objective of this study was to analyze temporal variations
95 in turbidity levels and chlorophyll content driven by sediment load, and to characterize long-term land
96 formation processes that resemble the “bird-foot” pattern in the MRD ecosystem.

97 2. Results and discussion

98 Figure 1 demonstrates the actual turbidity levels measured at USGS station 07374525 and the
99 corresponding NDTI values at the gauge location during 2013-2016 (The relevant data is given in the
100 supplementary data file). The fitted model demonstrates a strong linear relationship between NDTI and
101 turbidity levels. These results confirm that Landsat 8-derived NDTI values are accurate for predicting water
102 turbidity and sediment levels in the non-gauged Kitchen Pond area. The present analysis confirms the
103 accuracy of the developed remote sensing model for estimating water turbidity ($R^2 > 0.7$). This regression
104 model (Actual turbidity, FNU = $1664.5 * \text{NDTI} + 53.245$) can effectively predict actual turbidity levels based
105 on remotely sensed turbidity data (NDTI).



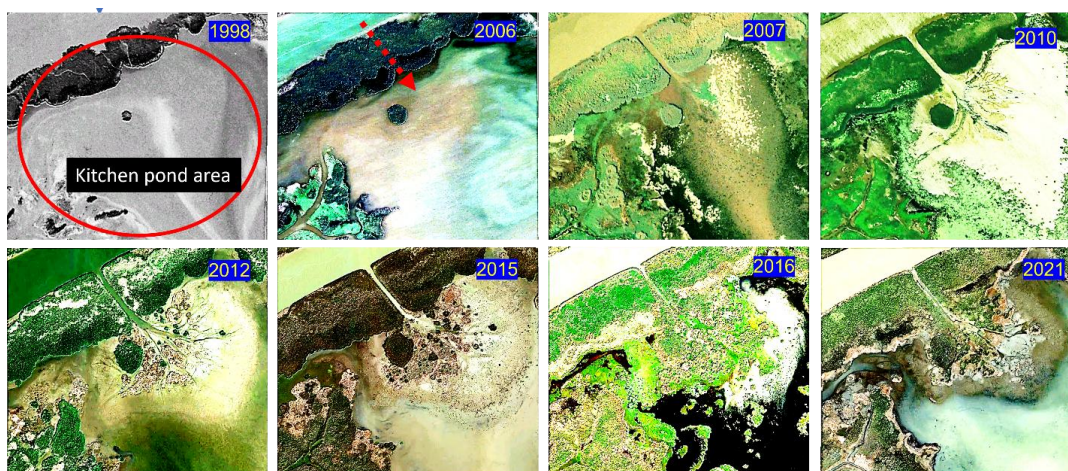
106 **Figure 1. Relationship between actual water turbidity and the NDTI values.**

107 Figure 2 illustrates the changes in sedimentation behavior in the Kitchen Pond area based on historical
108 imagery of Google Earth, after construction of the diversion canal in 2006-2007. Satellite images taken in
109 2007 (2007.07.22), 2009/2010 (2009.12.31), and 2012 (2012.10.29) clearly showed initial sediment
110 accumulation from the mouth of canal toward the Kitchen Pond. As observed from the image in 2012, a



111 sediment deposition pattern resembling a “bird’s foot” pattern is clearly visible, representing a typical
112 deltaic morphologic structure of the area. This pattern forms because the inlet water carries a large
113 amount of sediment which then accumulates at lower elevations, forming clogs forcing the flow to spread
114 out like fingers. Each of these fingers transports water and sediment outward to the low-lying water
115 bodies, in this case, the Kitchen Pond. The “bird’s foot” pattern is especially prominent when waves and
116 tides are too weak to erode or smooth out the new deposits, allowing each finger to continue expanding
117 outward independently (Edmonds and Slingerland, 2007). The conditions in the Kitchen Pond area are
118 highly favorable for this process to occur.

119 As shown in Figure 2, in 2021, a permanent landmass formed within the pond. providing potential for
120 above-ground vegetation to establish and persist. Thus, it can be established that 15 years after the
121 construction of the diversion canal, a permanent land mass occurred inside the pond as a result of
122 sediment deposition. This decadal timescale for stable land formation is consistent with observations from
123 other engineered sediment diversions in deltaic systems, such as those reported by (Kim et al., 2009), who
124 found that significant land emergence in the MRD often requires 10–20 years, depending on sediment
125 supply, hydrodynamics, and local basin conditions. This shows the effectiveness of sediment diversions in
126 deltaic land formation under favorable conditions. As shown by (Cahoon et al., 1995; Morris et al., 2002),
127 land formation proceeds through an initial rapid sedimentation phase followed by stabilization and
128 biomass increases. However, it is important to recognize that such positive outcomes are not always
129 possible. Day et al. (2009) and Kirwan et al. (2013) noted that land mass formation rates can be much
130 slower, or even negative, in areas with insufficient sediment supply, rapid sea level rise, strong erosional
131 forces etc. As evident by the present study, the 15-year development of a permanent landmass in Kitchen
132 Pond provides a valuable benchmark for restoration planning.

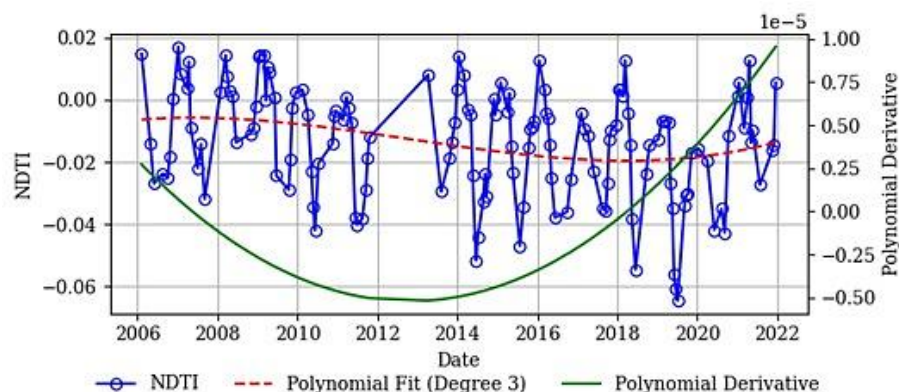


133 **Figure 2. Sediment deposition pattern and land formation in the kitchen pond area after the**
134 **construction of the diversion canal. The arrow in red indicates the newly constructed diversion canal in**
135 **2006-2007: Map data © 1998, 2006, 2007, 2010, 2012, 2015, 2016, 2021 Google.**



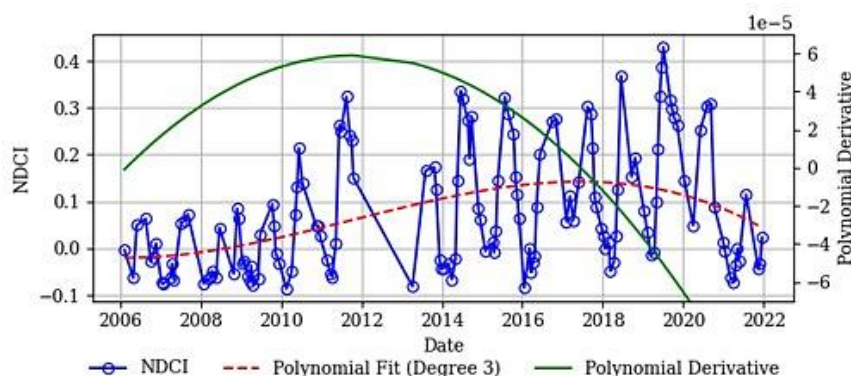
136 The google earth satellite images taken from year 2009/2010 (2009.12.31) and 2016 (2016.11.20) clearly
137 demonstrated the presence of floating vegetation on the water surface in the pond. Additionally, high
138 water turbidity was noted in the images from 2006 to 2012 (2006.3.14, 2007.7.22, 2009.12.31,
139 2012.10.29). This increase in turbidity could supply nutrients from the diversion canal for the growth of
140 newly arisen vegetation. This pattern is further evident by NDTI values variations during the study period.

141 Figure 3 depicts the temporal variations in turbidity levels in Kitchen Pond from 2006 to 2021 based on
142 the Landsat multitemporal imagery data (The relevant data is given in the supplementary data file).
143 According to the fitted polynomial trend line for NDTI, the turbidity levels in the pond were high in the
144 initial period (2007 to 2010) and then gradually declined. The minimum turbidity level was in 2019. From
145 2017 onwards, the turbidity trend reached approximately a constant level. The data gap from the 2012-
146 2013 period was due to the non-availability of satellite images for the study area. The annual decline of
147 NDTI was maximum in 2013 (1st order polynomial derivative).



148 **Figure 3. Temporal variation of NDTI in the water body in the Kitchen Pond.**

149 Figure 4 depicts the temporal variation of NDCI in the Kitchen Pond area. In contrast to NDTI, the NDCI
150 associated with the chlorophyll content in the pond showed a steady increase starting around 2009,
151 approximately 2-3 years after the construction of the diversion canal and continued the increasing trend
152 until 2018 (Figure 4). This increasing trend happened after the high turbidity event between 2007 to 2010.
153 The nutrient input associated with turbid water could create a favorable condition for the proliferation of
154 algae and floating vegetation. This increased vegetation biomass may have helped resist water flow across
155 the pond and enhance the sedimentation processes further.



156 **Figure 4. Temporal variation of NDCI in the water body in the kitchen pond.**

157 Debris of dead vegetation can be trapped efficiently during this phase and slow down the water flow
 158 through the submerged stems and roots, which concurrently could facilitate further sediment entrapment
 159 (Schile et al., 2014; Kirwan and Megonigal, 2013). This interaction is characterized by a positive feedback
 160 mechanism whereby the proliferation of vegetation is supported by increased sediment and nutrient
 161 availability, while the vegetation itself further accelerates and stabilizes land formation processes. As
 162 such, the newly emerged vegetation can be recognized as dependent on sediment and nutrient inputs but
 163 also actively involved in promoting further land accretion, positive feedback that strengthens both
 164 processes. As a result, the maximum rate of chlorophyll increase was observed as indicated by the
 165 polynomial derivative line constructed for NDCI in 2012 (Figure 4).

166 The current analysis indicates that the development of “bird-foot” like land formation is closely associated
 167 with sedimentation, nutrient input and emergence of vegetation in the low-lying water bodies. This
 168 highlights a dynamic interaction between hydrological and ecological processes, where changes in
 169 landform and vegetation influence each other, contributing to the ongoing evolution of the marsh
 170 ecosystem in the modern delta of the Mississippi River. However, recent studies have highlighted both
 171 the potential and the limitations of sediment-driven land formation in deltaic environments. For example,
 172 (Nienhuis et al., 2022) reported that man-made sediment diversions can lead to net land gain in certain
 173 deltas, which supports the observations made in this study in Kitchen Pond area following the construction
 174 of the diversion canal. However, it is important to note that the global trend is not always positive, as
 175 many deltas continue to experience land loss due to human activities and specific natural events. As
 176 indicated by (Morris et al., 2002), the ability of the vegetation to trap sediments and promote land
 177 formation is strongly influenced by the rate of sea-level rise or water level of the river during the flood
 178 season. In some cases, rapid sea-level rise can disturb sediment accumulation, resulting in marsh
 179 submergence rather than expansion. Kearney et al. (2002) also demonstrated that significant marsh loss
 180 can occur in regions where sediment supply or hydrological connectivity is disrupted.

181 The present analysis ensured a high level of accuracy and reliability in the results with the use of
 182 multitemporal Landsat imagery which is widely recognized for long-term environmental monitoring in
 183 wetland and deltaic systems, owing to its consistent revisit frequency. This makes it particularly effective
 184 for detecting gradual changes in water, sediment, and vegetation dynamics (Kearney et al., 2002; Kuenzer
 185 et al., 2011). Since the image database in GEE has already undergone standard preprocessing steps, such



186 as radiometric calibration, geometric correction, and atmospheric correction (Gorelick et al., 2017), the
187 analysis of turbidity and chlorophyll variations in this study is reliable.

188 3. Conclusion

189 This study successfully characterized the formation of landmass within a water body resulting from
190 sediment accumulation in the Kitchen Pond area in the modern delta of the Mississippi River using satellite
191 image analysis. The interaction between water turbidity driven by sediment supply, and the development
192 of vegetation on the emerging land mass was described. It was worth noting that nearly a 15-year period
193 was needed to form a permanent landmass by the sedimentation process under the conditions in the
194 Kitchen Pond area. The findings of this study provide valuable insights toward understanding how
195 sedimentation and natural succession of vegetation are involved in reshaping the landscape in the deltaic
196 ecosystem by providing real-world examples usable by coastal restoration agencies worldwide.

197 Appendix: Materials and Methods

198 The study was conducted in Kitchen Pond, located within the Modern delta of the Mississippi river, with
199 coordinates ranging from Latitude 29.203° to 29.210° and Longitude from -89.222° to -89.212° (Figure 5).

200 Landsat imagery from 2005 to 2021 was employed to analyze the water and land characteristics within
201 the study area. Images from 2022 onwards were excluded from the analysis due to the construction of
202 another diversion canal in the same area. All available Landsat images were visually inspected to identify
203 and exclude the ones affected by cloud contamination (The used Landsat image list is given in the
204 supplementary file “Supplementary_cloud free image list”). NDWI (Normalized Difference Water Index),
205 NDTI (Normalized Difference Turbidity Index), and NDCI (Normalized Difference Chlorophyll Index) were
206 estimated as defined by equations 1, 2, and 3. Cloud free 184 Landsat images were used. The computed
207 timeseries dataset of NDTI, NDCI and NDWI are given in the supplementary file
208 “Supplementary_NDTI.NDCI.NDWI”.

209
$$NDWI = \frac{G - NIR}{G + NIR} \dots\dots\dots \text{Eq 01 (McFeeters, 1999).}$$

210
$$NDTI = \frac{R - G}{R + G} \dots\dots\dots \text{Eq 02 (Garg et al., 2017).}$$

211
$$NDCI = \frac{NIR - R}{NIR + R} \dots\dots\dots \text{Eq 03 (Mishra and Mishra, 2012).}$$

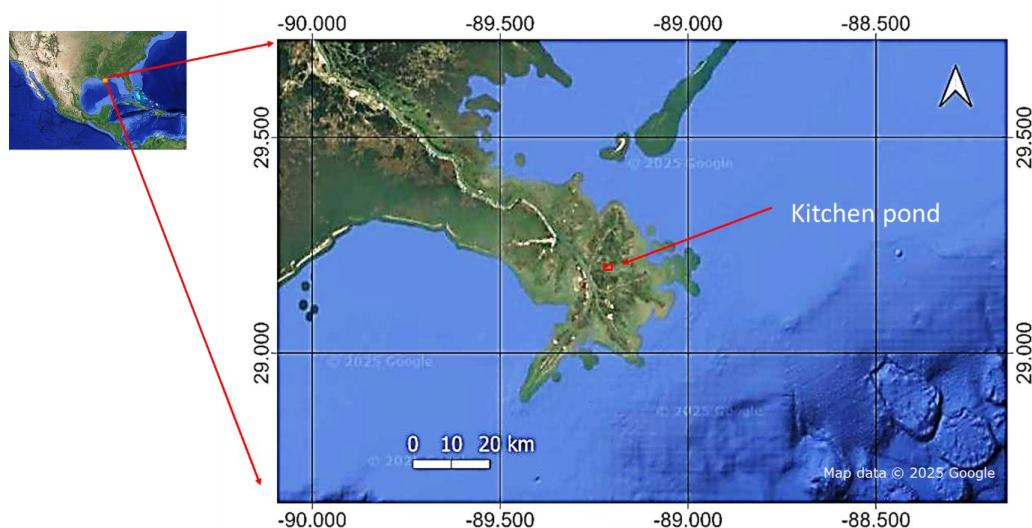
212 Where, G =green band, R = Red band, NIR = Near infrared band.

213 The NDWI, NDTI, and NDCI indices have been validated in numerous studies for delineating water bodies
214 (McFeeters, 1996), mapping turbidity (Garg et al., 2017), and estimating chlorophyll concentrations in
215 turbid waters (Mishra and Mishra, 2012), respectively. As the shape of the water body of Kitchen Pond
216 changed over the study period, precautions were taken to exclude ground pixels from water pixels in the
217 raster images by utilizing NDWI (Ortiz et al., 2017). The adoption of NDWI to separate water from land
218 pixels is consistent with best practices in remote sensing and helps minimize classification errors due to
219 seasonal or event-driven changes in pond morphology (Ji et al., 2009).

220 Image processing and data extraction were performed using Google Earth Engine (GEE) (Gorelick et al.,
221 2017). Google Earth Engine offers significant advantages in computational power and scalability allowing
222 for rapid processing of multiple satellite images without the need for local storage or high-end hardware.



223 By its default, the GEE imagery database has already undergone standard preprocessing steps, including
224 radiometric calibration, geometric correction, and atmospheric correction (Gorelick et al., 2017). Both
225 Landsat 5 and Landsat 8 images were used. Landsat 5 (8-bit radiometry) covers the period from 2005 to
226 2012, while Landsat 8 (12-bit radiometry) provides data from 2013 onwards. The spatial resolution of both
227 dataset is 30 meters. The code is available as a supplementary file (named “GEE code”).



228

229 **Figure 5. Study area in the Modern delta (bird-foot) of the Mississippi river: Map data © 2025 Google**

230 The NDTI, calculated from Landsat data, was validated using water turbidity measurements from the
231 Mississippi River at USGS station 07374525 (Mississippi River at Belle Chasse, LA). This station is the closest
232 to the study area, located approximately 101 km away on the Mississippi River at Belle Chasse, LA, with
233 coordinates 29.85715084°N, -89.97784700°W. USGS-07374525 turbidity data are available from
234 September 30, 2012 to June 20, 2016, total 2,587 daily data points. Based on satellite image availability,
235 30 data points where both turbidity measurements and satellite images were available were used for the
236 analysis. The dataset is given as a supplementary file “Suplimentary_turbidity data”.

237 **Data availability statement**

238 The data utilized in this study are available as suplimentary fiels in this paper and also publicly accessible
239 and can be downloaded online from “Mendeley data” web site. (Wijayawardhana, Janaka; Ratnayaka,
240 Harish (2026), “NDTI, NDCI, and NDWI data for the Kitchen Pond area in the Mississippi River Bird Foot
241 Delta.”, Mendeley Data, V2, doi: 10.17632/kczt6f37p.2)

242 **Author contributions**

243 L.M.J.R. Wijayawardhana contributed to research conceptualization, methodology development, coding,
244 data analysis, and manuscript writing. C.M. James and A.C. Jordan conducted satellite image analysis and
245 verification. H.H. Ratnayaka contributed to funding acquisition, method development, manuscript
246 improvements, and overall supervision.



247 **Competing interests.** Authors declare that none of the authors has any competing interests.

248 **Acknowledgment**

249 The authors would like to acknowledge the staff of the biology department of Xavier University of
250 Louisiana for their administrative support involved in the MissDelta project.

251 **Financial support**

252 This work was supported by the Gulf Research Program of the National Academies of Sciences,
253 Engineering, and Medicine under grant number SCON-10000883.

254 **Ethical declaration**

255 The authors declare that no ethical clearance was required for the publication of the content of this
256 manuscript.

257 **References**

258 Amer, R., Kolker, A.S. and Muscietta, A.: Propensity for erosion and deposition in a deltaic wetland
259 complex: Implications for river management and coastal restoration. *Remote Sensing of*
260 *Environment*, 199, 9-50, <http://dx.doi.org/10.1016/j.rse.2017.06.030>, 2017.

261 Barras, J.A.: Land area change in coastal Louisiana after the 2005 hurricanes: a series of three maps: U.S.
262 Geological Survey Open-File Report. 06-1274, 2006.

263 Cahoon, D.R., Reed, D.J. and Day Jr, J.W.: Estimating shallow subsidence in microtidal salt marshes of the
264 southeastern United States: Kaye and Barghoorn revisited. *Marine geology*, 128(1-2), 1-9,
265 [https://doi.org/10.1016/0025-3227\(95\)00087-F](https://doi.org/10.1016/0025-3227(95)00087-F), 1995.

266 Day, J.W., Cable, J.E., Cowan Jr, J.H., DeLaune, R., De Mutsert, K., Fry, B., Mashriqui, H., Justic, D., Kemp,
267 P., Lane, R.R. and Rick, J.: The impacts of pulsed reintroduction of river water on a Mississippi
268 Delta coastal basin. *Journal of Coastal Research*, 54(SI), 225-243, 2009.

269 Edmonds, D.A. and Slingerland, R.L.: Mechanics of river mouth bar formation: Implications for the
270 morphodynamics of delta distributary networks. *Journal of Geophysical Research: Earth Surface*,
271 112(F2), <https://doi.org/10.1029/2006JF000574>, 2007.

272 Garg, V., Kumar, A.S., Aggarwal, S.P., Kumar, V., Dhote, P.R., Thakur, P.K., Nikam, B.R., Sambare, R.S.,
273 Siddiqui, A., Muduli, P.R. and Rastogi, G.: Spectral similarity approach for mapping turbidity of an
274 inland waterbody. *Journal of hydrology*, 550, 527-537,
275 <https://doi.org/10.1016/j.jhydrol.2017.05.039>, 2017.

276 Geological Survey (USGS): Katrina_Rita_Coastwide Land Water: Assessment of land and water coverage
277 changes in coastal Louisiana within two months of Hurricanes Katrina and Rita. USGS Open-File
278 Report. 1274, 2006.

279 Gorelick, N., Hancher, M., Dixon, M., Ilyushchenko, S., Thau, D. and Moore, R.: Google Earth Engine:
280 Planetary-scale geospatial analysis for everyone. *Remote sensing of Environment*, 202, 18-27,
281 <https://doi.org/10.1016/j.rse.2017.06.031>, 2017.



- 282 Ji, L., Zhang, L., and Wylie, B.K.: Analysis of dynamic thresholds for the normalized difference water index:
283 Photogrammetric Engineering and Remote Sensing, v. 75, no. 11, 1307-1317,
284 <https://doi.org/10.14358/PERS.75.11.1307>, 2009.
- 285 Kearney, M.S., Rogers, A.S., Townshend, J.R., Rizzo, E., Stutzer, D., Stevenson, J.C. and Sundborg, K.:
286 Landsat imagery shows decline of coastal marshes in Chesapeake and Delaware Bays. *Eos*,
287 *Transactions American Geophysical Union*, 83(16), 173-178.
288 <https://doi.org/10.1029/2002EO000112>, 2002.
- 289 Kim, W., Mohrig, D., Twilley, R., Paola, C., & Parker, G.: Is it feasible to build new land in the Mississippi
290 River delta? *EOS Transactions, American Geophysical Union*, 90, 373-384,
291 <https://doi.org/10.1029/2009EO420001>, 2009.
- 292 Kirwan, M.L. and Megonigal, J.P.: Tidal wetland stability in the face of human impacts and sea-level
293 rise. *Nature*, 504(7478), 53-60, <https://doi.org/10.1038/nature12856>, 2013.
- 294 Kuenzer, C., Bluemel, A., Gebhardt, S., Quoc, T.V. and Dech, S.: Remote sensing of mangrove ecosystems:
295 A review. *Remote Sensing*, 3(5), 878-928, <https://doi.org/10.3390/rs3050878>, 2011.
- 296 McFeeters, S.K.: The use of the Normalized Difference Water Index (NDWI) in the delineation of open
297 water features. *International journal of remote sensing*, 17(7), 1425-1432,
298 <https://doi.org/10.1080/01431169608948714>, 1996.
- 299 Mishra, S. and Mishra, D.R.: Normalized difference chlorophyll index: A novel model for remote estimation
300 of chlorophyll-a concentration in turbid productive waters. *Remote Sensing of Environment*, 117,
301 394-406, <https://doi:10.1016/j.rse.2011.10.016>, 2012.
- 302 Morris, J.T., Sundareshwar, P.V., Nietch, C.T., Kjerfve, B. and Cahoon, D.R.: Responses of coastal wetlands
303 to rising sea level. *Ecology*, 83(10), 2869-2877, 2002.
- 304 Nienhuis, J. H., Ashton, A. D., Edmonds, D. A., Hoitink, A. J. F., Kettner, A. J., Rowland, J. C., Tornqvist, T.
305 E.: Global-scale human impact on delta morphology has led to net land area gain. *Nature*, 577,
306 <https://doi.org/10.1038/s41586-022-05079-0>, 2022.
- 307 Ortiz A.C, Roy S, Edmonds DA.: Land loss by pond expansion on the Mississippi River Delta Plain.
308 *Geophysical Research Letters.*, 44(8):3635-42, <https://doi:10.1002/2017GL073079>, 2017.
- 309 Sanks, K.M., Zapp, S.M., Silvestre, J.R., Shaw, J.B., Dutt, R. and Straub, K.M.: Marsh sedimentation controls
310 delta top morphology, slope, and mass balance. *Geophysical Research Letters*, 49(12),
311 2022GL098513, <https://doi.org/10.1029/2022GL098513>, 2022.
- 312 Schile, L.M., Callaway, J.C., Morris, J.T., Stralberg, D., Parker, V.T. and Kelly, M.: Modeling tidal marsh
313 distribution with sea-level rise: evaluating the role of vegetation, sediment, and upland habitat in
314 marsh resiliency. *PloS one*, 9(2), 88760, doi: 10.1371/journal.pone.0088760, 2014.
- 315 Syvitski, J.P. and Saito, Y.: Morphodynamics of deltas under the influence of humans. *Global and Planetary*
316 *Change*, 57(3-4), 261-282, <https://doi.org/10.1016/j.gloplacha.2006.12.001>, 2007.
- 317 Xu, Y., Esposito, C.R., Beltrán-Burgos, M. and Nepf, H.M.: Competing effects of vegetation density on
318 sedimentation in deltaic marshes, *Nature Communication.*, 13, 4641,
319 <https://doi.org/10.1038/s41467-022-32270-8>, 2022.